Desalination and Water Treatment
www.deswater.com

doi: 10.5004/dwt.2019.24236

161 (2019) 188–202
September

Colour removal from industrial wastewater using acid-modified tea leaves, a domestic waste

Shubhrajit Sarkar[a], Santanu Sarkar[b], Samya Subhra Das[a], Chiranjib Bhattacharjee[a,*]

[a]*Chemical Engineering Department, Jadavpur University, Kolkata, India, emails: c.bhatta@gmail.com (C. Bhattacharjee), sarkarshubhrajit@gmail.com (S. Sarkar), samyasubhra@gmail.com (S.S. Das)*
[b]*Environment Research Group, R&D, Tata Steel Ltd., Jamshedpur, India, email: ssarkar05@gmail.com*

Received 23 November 2018; Accepted 6 April 2019

ABSTRACT

The dye-containing wastewater discharged from various industries such as textile, paint, paper, cosmetic, dye producing, etc. severely contaminate surface water and have detrimental effect on the environment as well as living organisms. In this present study, novel acid-modified tea leaves (AMTL) were synthesized from used tea leaves and used as a cost-effective biosorbent to remove anionic dye (Reactive Green 19, RG 19) from the effluent stream. The biosorbent was characterized by thermogravimetry, X-ray diffraction, Fourier transform infrared and scanning electron microscopy. Batch experiments for dye adsorption were carried out to analyse biosorbent dose, pH, stirring speed, temperature, contact time and initial dye concentration. Langmuir, Freundlich and Temkin isotherms were implemented to investigate and fit batch experimental data. The adsorption of RG 19 has followed Langmuir isotherm ($R^2 > 0.988$) with maximum adsorption capacity of 26.316 mg g^{-1}. Biosorption kinetics of RG 19 by AMTL has followed pseudo-second-order kinetic model ($R^2 > 0.999$). The values of $\Delta G°$ (–1.66 to –5.94 kJ mol^{-1}) and $\Delta H°$ (70.764 kJ mol^{-1}) demonstrated that the adsorption of RG 19 was spontaneous endothermic process.

Keywords: Biosorption; Reactive Green 19; Acid-modified tea leaves; Isotherms; Adsorption kinetics; Stirring speed

1. Introduction

A large amount of wastewater containing different types of dyes are discharged from textile, dye producing, cosmetic, leather, pulp and paper, plastic and rubber, and pharmaceutical industries [1,2]. Nowadays more than 10,000 types of commercial dyes are available in the market and around 7×10^5 tons of dyes are produced yearly worldwide and used widely in various industries for several purposes [3]. It has also estimated that around 10%–15% of total dyes is lost in the various industrial effluent streams [4], thereby polluting the environment adversely.

Among all kinds of dye, the textile dyes have harmful effects on human as well as animal health, such as malfunction of kidneys, disorder in reproductive system, liver, brain, and the central nervous system due to their toxic, carcinogenic and mutagenic nature [5,6]. The existence of very small amount (10–50 mg L^{-1}) of dye in water can even reduce the sunlight penetration into water and cause hindrance in the photosynthesis process, thus disturbing aquatic equilibrium as well as the food chain [7,8]. Hence, the removal of colourful dyes from the industrial effluent becomes a major concern in context to environmental aspects, demanding urgent attention in such lucid area. Different conventional technologies have been used for the removal of dyes from the waste stream, which include biodegradation [9], heterogeneous photocatalytic degradation [10], solar photo-Fenton degradation [11], photo-Fenton processes [12], electrochemical degradation [13], hybrid chemical–biological degradation [14,15] and adsorption [16,17]. Traditional biodegradation

* Corresponding author.

techniques are not efficient for textile wastewater treatment due to the lower biodegradability of dyes [18]. Moreover other technologies are not economically viable due to their higher operating cost. The biosorption process for wastewater treatment has gained great attention in recent times due to their low operational cost [19]. Moreover, the conventional biosorbents can be easily modified to increase adsorption capacity [20]. Hence, the adsorption of dyes from wastewater in the presence of biosorbents becomes an effective technology. Consequently, several researchers have attempted to develop cost-effective adsorption techniques for removal of colour from wastewater. In order to fulfill this purpose, several materials such as chitosan [21], mango seed kernel dust [22], neem saw powder [23], modified rice straw [24], activated carbon produced from groundnut shell waste [25], clay [26], calcium-rich fly ash [27], etc. have been investigated. The researchers have shown major interest to find out suitable biosorbent for anionic dye adsorption from effluent stream as the adsorption capacities of most of the aforementioned biosorbents for removal of anionic dyes are not appreciable.

However, the uses of normal plant or agricultural wastes have some difficulties during adsorption process such as extremely low adsorption capacity, high biological and chemical oxygen demand. In some cases, the total organic carbon (TOC) value also increases due to the release of organic compounds present from the unmodified plant wastes [28]. Therefore, different chemical techniques have been used for the activation or modification of biosorbents, such as $ZnCl_2$ [28], KOH [29], SDS [30] and H_3PO_4–$NaHCO_3$ [31]. H_3PO_4 has been commonly used as an activating agent for biosorbent preparation from lignocellulosic material and it can be easily separated by water and also offers non-polluting characteristic [32,33].

Several types of agricultural wastes are generated worldwide in bulk quantity. Among them, tea waste is one of the major contributors of such type of waste. India produces 1,112 million kg of tea annually from the tea plant called *Camellia sinensis* and is the second largest manufacturer of tea in the world. It constitutes about 24.56% of worldwide tea production [34]. However, used tea leaves create serious disposal problem due to its oxygen demanding nature and lower biodegradability. To mitigate limitations regarding disposal of tea leaves several initiatives have been taken so far to utilize those used tea leaves as a natural biosorbent. For instance the used tea leaves can easily adsorb heavy metals [35] or dyes [36] from waste stream and modified waste tea leaves has greater biosorption activity than unmodified one. After adsorption, tea wastes become saturated and then it is finally incinerated. Ash generated by the incineration of saturated tea waste can be used as a biosorbent instead of recognizing it as an environmental pollutant [36]. Henceforth, in the present research work, acid-modified tea leaves (AMTL) waste has been selected as biosorbent for the removal of dye (RG 19) from its aqueous solution.

The current study focuses on the application of AMTL waste for dye of RG 19 removal from its aqueous solution. The novelties of the current work are very specific and straight forward, that is, the modification of used tea leaves and its utilisation for the removal of anionic dye from wastewater. So far, there is no publication available for anionic dye, RG 19, removal by adsorption using AMTL waste. Moreover, the effects of process parameters such as biosorbent dose, pH and temperature of the solution, shaking speed and residence time were studied and several adsorption isotherms, that is, Langmuir, Freundlich and Temkin were verified with the experimental data. Finally, adsorption kinetic parameters were estimated and their variations with different initial dye concentrations were depicted here.

2. Materials and methods

2.1. Reactive Green 19 (RG 19)

RG 19, $C_{40}H_{23}Cl_2N_{15}Na_6O_{19}S_6$, having molecular weight 1,418.94, which was supplied by Sigma-Aldrich, USA (CAS NO. 61931-49-5 and λ_{max} = 630 nm), was used as adsorbate for this study. The structure of RG 19 is illustrated in Fig. 1.

2.2. Preparation of biosorbent

Raw used tea leaves were collected from a canteen located in the campus of Jadavpur University, Kolkata, India. Initially used tea leaves were boiled with purified water repeatedly until the filtered water became colourless. Then it was boiled with 30% H_3PO_4 for 30 min and retained in same acid solution for 24 h. Acid-treated waste tea leaves were repeatedly washed with water until its pH became neutral. After that, it was dried in the oven at 80°C for 24 h. The dried AMTL were grounded and sieved to obtain particle size of 250 μm and below. Finally, biosorbent was stored in airtight plastic container for future use.

2.3. Adsorption study

The whole batch adsorption study was carried out in a 250 mL stoppered glass Erlenmeyer's flask with 100 mL working solution for 120 min. During the adsorption, the temperature was kept constant with the help of temperature-controlled shaker at constant shaking speed of 175 rpm. After adsorption, the samples were withdrawn and centrifuged at 10,000 rpm for 10 min to separate biosorbent from the working solution. Then dye concentrations of the

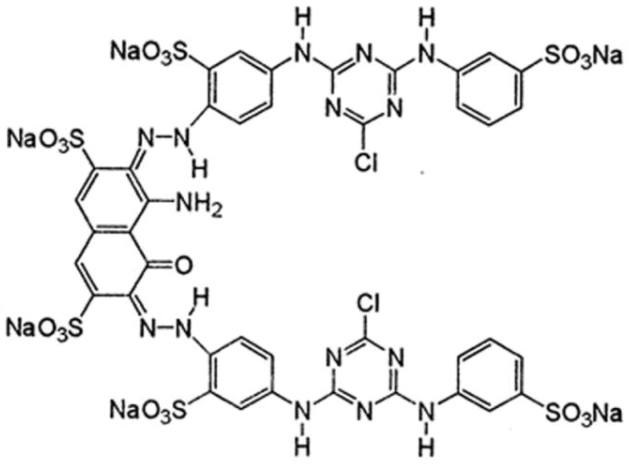

Fig. 1. Molecular structure of RG 19.

supernatant were measured by UV–Vis spectrophotometer (Model: Varian Cary 50Bio and Part no: EL07113760) at 630 nm wavelength.

To study the effect of modified biosorbent dose for the removal of reactive RG 19, weight of AMTL were varied from 0.1 to 1.2 wt.% when dye concentration was maintained at 100 ppm. As pH played an important role for dye adsorption, pH of working solution was varied in the range from 2 to 10. The pH of the dye solution was adjusted at desired value using 0.1 N NaOH and 0.1 N HCl solutions. pH of the solutions were measured by digital pH meter (Hanna, Romania). During the pH variation, 100 ppm of the dye solution was stirred with 0.8 wt.% of AMTL at constant temperature of 30°C. Moreover, the effect of temperature and agitation on adsorption was measured with variation of temperature from 25°C to 40°C and shaking speed from 100 to 200 rpm, respectively, when all other parameters were kept constant. All the experiments were performed in triplicate sets.

2.4. Equilibrium studies

Equilibrium studies were carried out for 120 min with variation of initial dye concentrations in the range of 50–300 ppm at constant optimized conditions, that is, biosorbent concentration (0.8 wt.%), temperature 30°C and pH 3. Samples were withdrawn after certain time interval and centrifuged to measure dye concentrations. Trial experimental run confirmed that to reach the equilibrium condition, residence time of 120 min should be maintained. The equilibrium biosorption, q_e (mg g^{-1}) was calculated by Eq. (1).

$$q_e = \frac{\left(C_0 - C_e\right)}{W} \times V \tag{1}$$

where C_0 and C_e (ppm) are the liquid phase concentration of RG 19 at initial and equilibrium condition, respectively. V (L) is the initial volume of dye solution and W (g) is the weight of the biosorbent used.

Equilibrium dye removal percentage was calculated using the equation below.

$$\text{Removal percentage} = \frac{\left(C_0 - C_e\right)}{C_0} \times 100 \tag{2}$$

2.5. Batch kinetic studies

The method for batch adsorption kinetics study was similar to the equilibrium studies. However, samples were collected at fixed time interval and the concentrations of dye were measured. The amount of dye adsorbed at any time t, q_t (mg g^{-1}) was calculated by the following relationship:

$$q_t = \frac{\left(C_0 - C_t\right)}{W} \times V \tag{3}$$

where C_t denotes the liquid phase dye concentration at any time t.

2.6. Statistical analysis

The statistical analysis of the experimental data was conducted carried out by one-way ANOVA using Minitab 16. The confidence level (CI) for evaluating statistical significance was considered as 95%.

3. Results and discussions

3.1. Effect of biosorbent dose on dye adsorption

The biosorbent dose was varied to determine the optimum amount of biosorbent required for dye removal. In this study, 100 mL of 100 ppm dye solution was taken and the amount of biosorbent was varied. Fig. 2 shows the effect of both raw and modified used tea leaves (AMTL) dose on the percentage removal of RG 19. The results manifest that the modification of raw tea leaves has promoted the dye adsorption mechanism leading to the increase in the removal percentage compared with raw used tea leaves. Relative standard deviation between the percentage removal by raw and modified tea leaves was found sufficiently high (about 25.1%) indicating significant deviation in adsorption capacity of raw used tea leaves and AMTL. It was found that the percentage removal of dye was increased with the increase in the amount of biosorbent dose due to the availability of more active surfaces and sites for enhanced biosorption. At the equilibrium percentage removal of dye increased from 43.7% to 95.9% by increasing the amount of biosorbent with the limiting value of 0.8 g. The mentioned quantity (0.8 g in 100 mL working solution) is evaluated as the optimal biosorbent dose as the percentage removal of dye remains unchanged with any further increase of biosorbent dose. The percentage removal of RG 19 gradually increases with the increase in biosorbent dose up to 0.8 g/100 mL of solution because of the enhanced availability of biosorption sites and increased surface area with the increase in biosorbent dosage. However, no further change or improvement in the percentage removal of RG 19 has been found beyond 0.8 g/100 mL. It can be attributed to the fact that at very high biosorbent dose beyond 0.8 g, saturation point is reached due to overlapping or aggregation of biosorbent particles, ultimately reducing the availability of biosorption sites,

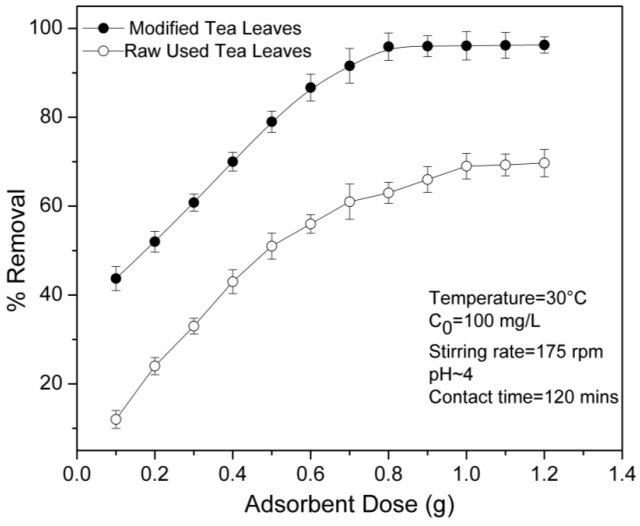

Fig. 2. Effect of biosorbent dose on the adsorption of RG 19 on both raw used tea leaves and acid-modified tea leaves (AMTL).

surface area of the biosorbent and increasing the diffusion path length [37]. Though till date only a few researches had been carried out on RG 19 adsorption, a literature comparison was highlighted in Table 1 in terms of removal efficiency of RG 19 using different types of biosorbent. This table manifests the well suitability of AMTL as biosorbent for efficient removal of dye RG 19.

3.2. Effect of solution pH on dye adsorption

The effect of pH on the biosorption of RG 19 is shown in Fig. 3. To understand the effect of the pH on dye removal, the pH of the solution was varied from 2 to 11 with constant dye concentration (100 ppm) and optimal biosorbent dose of 0.8 g/100 mL. Since RG 19 is an anionic dye, it remains negatively charged in the aqueous solution. As a result, the adsorption mechanism of RG 19 on the biosorbent surface is being governed by surface charge of the biosorbent, which is greatly affected by the pH of the solution. Fig. 3 indicates that the percentage removal of dye was maximum at pH 3 (95.9%) and it remained constant over the pH range of 4–5. It was found that the equilibrium dye adsorption (q_e) decreases with the increasing pH. The equilibrium biosorption of dye is higher in acidic range (at low pH) because of the presence of excess H^+ ions, which shows high affinity to bind or combine with negatively charged anionic dye and thus facilitates the anionic dye biosorption process. Similar type of result was found for anionic dye CR removal by *Myrtus communis* and pomegranate [41]. The statistical result shows that the *F*-value, defined as the variance in group means over mean of the variance within the group, is 118.34 ($>F_{Critical}$ = 4.49) between the groups. Such a large *F*-value manifests that there is significant deviation in RG 19 uptake by adsorbent in the pH range of 2–10. Moreover small *p* value ($p < 0.05$) also suggests that pH is a significant parameter that affects the removal percentage of dye with its slight variation.

3.3. Effect of stirring speed on dye adsorption

The effect of stirring speed was also studied by varying the shaking speed in the range of 100–200 rpm with a constant initial dye concentration of 100 ppm, optimum biosorbent dose of 0.8 g/100 mL, and pH 3. The results have been plotted in Fig. 4a. The figure clearly explains that the dye removal percentage increases with increase in stirring speed of the system. The mechanism for dye removal (shown in Fig. 4b) from the effluent involves four steps such as initially the dye(s) molecules migrates from the liquid phase to the boundary layer that is formed on the outer surface of the biosorbent; in the next step the diffusion of the adsorbate through the boundary layer takes place, then biosorption of dye molecules at the outer side of the biosorbent occurs and the final step is the intraparticle diffusion of the adsorbate into the interior part of the biosorbent. Henceforth the increase in the biosorption of dye with the increase in shaking speed is because of the alteration in resistance of the boundary layer. The boundary layer resistance decreases with increase in shaking speed and hence the rate of diffusion or the mobility of the dye(s) molecules increases in the system [42]. Eventually, the dye(s) molecules are forced to move towards the biosorbent surfaces causing increment in the adsorption rate [42,43]. Moreover ANOVA was carried out to validate statistically the experimental data obtained at equilibrium conditions. It was observed that the *F*-value (9.615)

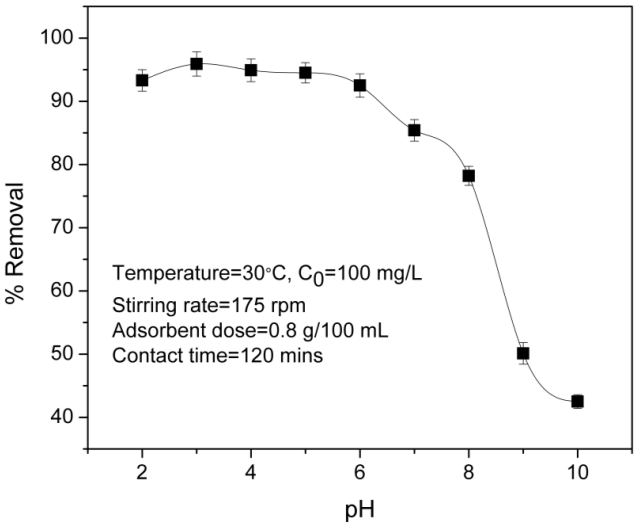

Fig. 3. Effect of solution pH on the adsorption of RG 19 on AMTL.

Table 1
Literature comparison of RG 19 adsorption using different types of biosorbent

Adsorbent	Initial RG 19 concentration (mg L^{-1})	Dye removal percentage (%)	Residence time (min)	References
Untreated spent black tea leaves	50	6.75	60	[38]
Modified spent black tea leaves (after thermal activation to 300°C for 1 h)	50	98.8	60	[38]
Activated carbon	50	77	60	[38]
Fuller's earth	50	8	60	[38]
Ground nut shell carbon (GNC)	40	78.5	60	[39]
Baby corn carbon (BCC)	40	79	60	[39]
Peanut shell powder	250	96.3	90	[40]
Acid-modified tea leaves (AMTL)	100	95.9	20	Present study

is greater than $F_{Critical}$ (5.32) revealing the rejection of null hypothesis, that is, significant change in RG 19 adsorption with the variation in shaking speeds. Moreover, low *p*-value ($p < 0.05$) also confirms that shaking speed (rpm) is a significant parameter affecting the adsorption of dye by AMTL.

3.4. Effect of temperature on dye adsorption and thermodynamic study

To evaluate the effect of temperature on biosorption process, the biosorption experiments were carried out at four different temperatures such as 20°C, 25°C, 30°C and 35°C, with constant dye concentration of 100 ppm, optimum AMTL dose of 0.8 g/100 mL and pH of 3. It was also found from Fig. 5a that the amount of RG 19 adsorbed by AMTL increased with increase in temperature. The results indicate that biosorption of RG 19 on AMTL surfaces is an endothermic process and such observation is an exceptional phenomenon. However, several researchers also have found that biosorption of reactive dye by different biosorbents was endothermic [10,44,45]. The statistical analysis shows that the determined *F*-value (364.84) is higher than $F_{Critical}$ (5.98) and *p*-value (0.000006) is quite below the confidence interval. Such a large *F*-value and low *p*-value reveals the non-applicability of null hypothesis. Thus significant deviation in RG 19 adsorption by AMTL at equilibrium condition was observed with the change in temperature, indicating the temperature as a significant parameter in controlling the adsorption phenomenon.

The thermodynamic properties of the dye adsorption process, $\Delta S°$, $\Delta G°$ and $\Delta H°$, were calculated by using equations as mentioned below [46]:

$$\Delta G_0 = -RT\ln K \tag{4}$$

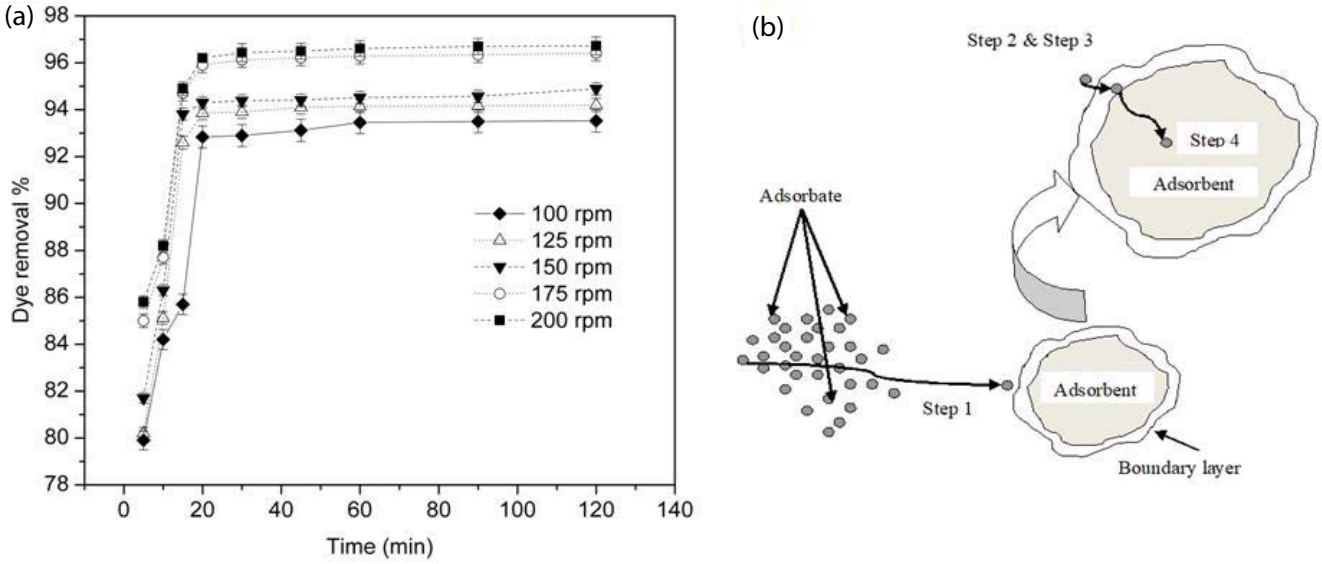

Fig. 4. (a) Effect of agitation speed on the removal of RG 19 on AMTL and (b) mechanism of dye adsorption on AMTL.

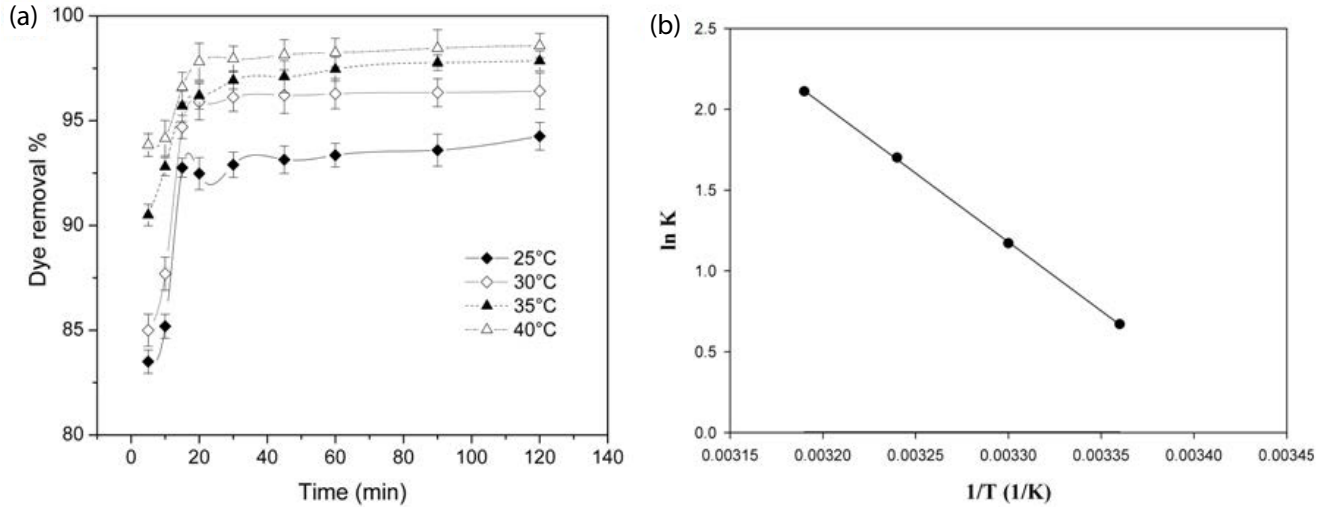

Fig. 5. (a) Effect of temperature on the removal of RG 19 on AMTL and (b) plot of ln *K* vs 1/*T* for the adsorption of RG 19 on AMTL.

$$\ln K = \frac{\Delta S^0}{R} - \frac{\Delta H}{RT} \quad (5)$$

$$K = \frac{q_e}{C_e} \quad (6)$$

where $\Delta S°$, $\Delta G°$ and $\Delta H°$ are the standard entropy change, standard Gibbs free energy change and standard enthalpy change. R is the universal gas constant (8.314 J mol^{-1} K^{-1}), T denotes the temperature in Kelvin and K denotes the distribution coefficient of the adsorbate. All the mentioned relationships (Eqs. (4)–(6)) are valid when the change in enthalpy remains constant in the temperature range.

Fig. 5b shows that ln K vs. $1/T$ is a linear plot. The intercept and slope gives the values of ΔS and ΔH. The thermodynamic parameters for 100 ppm dye solution were calculated and listed in Table 2. From the table, it can be observed that ΔH value for biosorption of RG 19 was positive, manifesting the endothermic nature of biosorption phenomenon. Moreover the positive value of ΔS indicated the gradual increase in the randomness at the solid/solution interface during the course of biosorption process of dye RG 19 onto AMTL. Furthermore, the free energy changes (ΔG) at varied temperatures were found negative, revealing the thermodynamically spontaneous nature and feasibility of RG 19 biosorption process. Again from Table 2, it is clearly understandable that the negative ΔG values follow a decreasing trend with the increase in temperature which further confirms the suitability and spontaneity of biosorption of dye on the AMTL. It was found from previous researches that the adsorption energies for physical and chemical adsorption were in the range of 0 to −20 kJ mol^{-1} and −80 to −400 kJ mol^{-1}, respectively [47]. In the present study, the adsorption energies varied in the range of –1 to –6 kJ mol^{-1} indicating the physical biosorption nature of the process. The physical biosorption generally occurs when the intermolecular attractive forces between the biosorbent and adsorbate becomes stronger than the intermolecular forces within the adsorbate molecules. On the other hand, chemisorption process follows the chemical bonds formation within the molecules of biosorbent and adsorbate. Therefore it can be concluded that the present biosorption study of RG 19 on AMTL followed a physical biosorption mechanism.

3.5. Effect of contact time and initial concentration on dye adsorption

Fig. 6 shows the effects of initial dye concentration (50–300 ppm) on the removal of RG 19 by the biosorbent with varying contact time. The amount of dye adsorbed per unit mass of the biosorbent increased with the increasing initial dye concentration, although the percentage removal of dye decreased. The amount of dye adsorbed at equilibrium (q_e) was elevated from 5.923 to 26.24 mg g^{-1} with the increase in the initial dye concentration from 50 to 300 ppm. However, it was also observed that the equilibrium percentage removal of RG 19 decreased from 98.718 to 72.89 as the initial dye concentration increases from 50 to 300 ppm. As the mass transfer resistance becomes larger with the increase of initial dye concentration in the solution, the percentage removal of dye gradually decreases, though the amount of RG 19 adsorption increases with initial dye concentration. It was also found that as the time progresses, the removal of RG 19 has increased for each initial dye concentration and ultimately reached its equilibrium point.

Fig. 6 shows rapid adsorption of RG 19 in the first 20 min for all initial dye concentration. After that the adsorption rate of dye decreases and finally reaches equilibrium. The residence time required to achieve equilibrium for initial dye concentration of 50–150 ppm and 200–300 ppm was 20 and 30 min, respectively. However, the experiments were performed for 120 min to become confirmed that the complete equilibrium was reached.

Table 2
Thermodynamic parameters for the adsorption of RG 19 on AMTL at different temperatures

Temperature (°C)	$\Delta G°$ (kJ mol^{-1})	$\Delta H°$ (kJ mol^{-1})	$\Delta S°$ (kJ mol^{-1})
25	–1.66	70.764	0.243
30	–2.95		
35	–4.35		
40	–5.94		

3.6. Effect of ionic strength on dye adsorption

Addition of inorganic salts is very common in the course of dyeing mechanism utilizing reactive dyes, to promote the bonding between dye and fiber by forcing the dye molecules out of the bulk solution onto the fiber surface. Henceforth, two widely utilized inorganic salts, sodium chloride (NaCl) and sodium sulphate (Na_2SO_4) were selected to evaluate the ionic effects of these salts on RG 19 adsorption mechanism. From Fig. 7 it was observed that the incorporation of NaCl at dosage of 0.1 to 0.5 M resulted in the increase of RG 19 uptake. However, no further elevation in RG 19 uptake was found beyond the low concentration of NaCl (0.1 M).

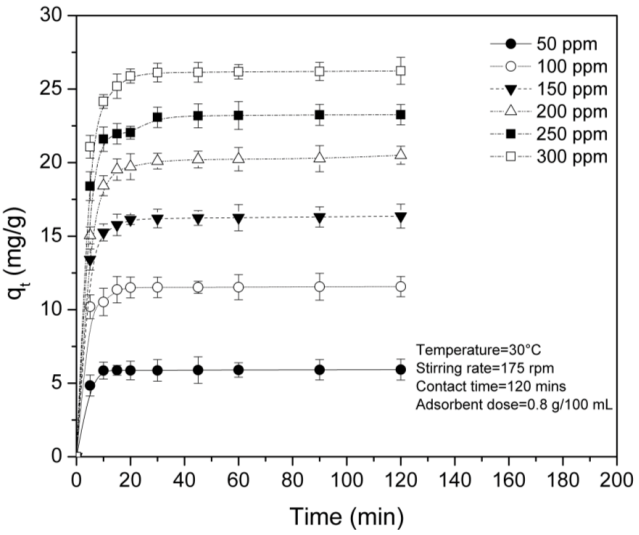

Fig. 6. Effect of contact time and initial concentration of RG 19 adsorption on AMTL.

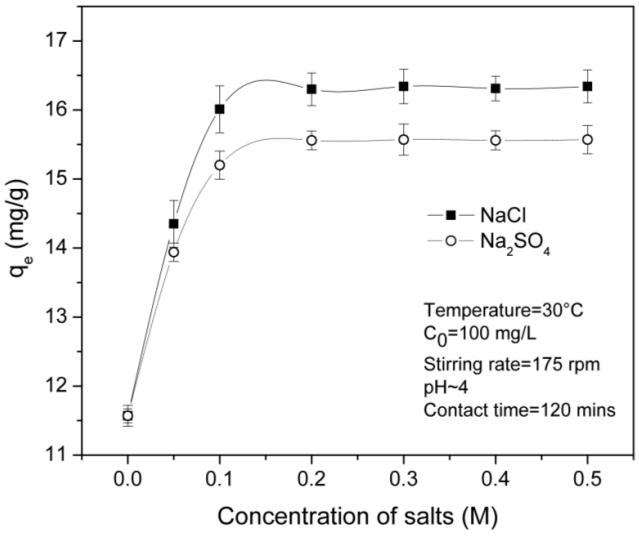

Fig. 7. Effect of ionic strength on adsorption capacity of AMTL.

Similar result was also observed on addition of Na_2SO_4 salt. From the theoretical point of view, when the electrostatic forces of attraction is predominant between the biosorbent surface and adsorbate ions, the adsorption capacity will be reduced with the rise in ionic strength [48,49]. However the present experimental data showed the reverse trend as with the addition of Na salts, the adsorption of anionic dye molecules was facilitated on positively charged biosorbent surface leading to the substantial enhancement in dye removal. This is attributed to the exaggerated aggregation of dye molecules because of the induced action of salt ions to increase several intermolecular forces such as Van der Waals forces, dipole–dipole forces and ion–dipole forces acting in between the dye molecules in the solution [49,50]. From the statistical ANOVA analysis, it can be interpreted from very high *F*-value and low *p*-value that ionic strength is also a significant parameter that controls the uptake of RG 19 dye by AMTL. *F*-values (485.59 and 637.68) were found sufficiently greater than $F_{critical}$ (4.75) for both NaCl and Na_2SO_4, respectively, and *p* values were very less, thus rejecting the null hypothesis validation.

3.7. Isotherm analysis

Langmuir, Freundlich and Temkin isotherms were used to analyse the suitable isotherm for RG 19 adsorption on AMTL. In case of any adsorption analysis, the determination of suitable isotherm using equilibrium data at room temperature (30°C) is of utmost importance [19].

3.7.1. Langmuir isotherm

The Langmuir [52] isotherm (Fig. 8a) is the simplest model for physical adsorption. The assumptions of this model are (i) the molecules are adsorbed at separate active sites on the surface, (ii) only one molecule is adsorbed at each active site, (iii) energy of the adsorbing surface is uniform and (iv) adsorbed molecules cannot interact with each other [51,52]. The Langmuir isotherm can be linearised according to Eq. (7).

$$\frac{C_e}{q_e} = \frac{C_e}{q_m} + \frac{1}{\left(K_L q_m\right)} \tag{7}$$

where q_m (mg g^{-1}) is the maximum adsorption capacity of AMTL and the Langmuir isotherm constant K_L (L mg^{-1}) is related to the adsorption energy. The values of different constants were determined using the equilibrium data and Langmuir isotherm equation and values are tabulated in Table 3.

The important characteristic of Langmuir isotherm can be articulated in terms of a dimensionless constant called separation factor (R_L) which is calculated as follows [53].

$$R_L = \frac{1}{\left(1 + K_L C_0\right)} \tag{8}$$

where C_0 is the initial adsorbate concentration and K_L is the Langmuir isotherm constant. Depending on the values of R_L, suitability of process can be evaluated likely the process is unfavourable ($R_L > 1$), linear ($R_L = 1$), favourable ($0 < R_L < 1$) or irreversible ($R_L = 0$) [53]. Favourable adsorption occurs when the values of R_L are in between 0 and 1. R_L values for the adsorption of RG 19 by AMTL were in between the range of 2.79×10^{-3} and 4.672×10^{-4} for initial dye concentration of 50–300 ppm, respectively, which signifies the favourability of adsorption of RG 19 on AMTL surface. Adsorption process becomes irreversible with increasing initial dye concentration.

3.7.2. Freundlich isotherm

The Freundlich isotherm (Fig. 8b) is an empirical isotherm which assumes that the quantity adsorbed at equilibrium has a power law dependence on the concentration of the solute [54].

The Freundlich isotherm can be linearised as follows:

$$\ln q_e = \ln K_f + \frac{1}{n} \ln C_e \tag{9}$$

where K_f and n denotes Freundlich isotherm constants. K_f (mg g^{-1}) (L $mg^{-1})^{1/n}$ is associated with biosorption capacity and $1/n$ is related to adsorption intensity. The value of $1/n$ gives an idea about the favourability of adsorption. Value of $n > 1$ implies that the adsorption process is favourable [55]. The values of Freundlich isotherm constants and linear regression correlation for Freundlich model are given in Table 3.

3.7.3. Temkin isotherm

In case of Temkin isotherm (Fig. 8c), the effects of some indirect interactions between adsorbate molecules on adsorption isotherms were considered and suggested that the heat of adsorption of all the molecules in the layer would decrease linearly with coverage due to these interactions. The Temkin isotherm can be linearised according to Eq. (10).

$$q_e = B \ln A + B \ln C_e \tag{10}$$

where the constant $B = RT/b$ is associated with the heat of adsorption, R is universal gas law constant (8.314 J K^{-1} mol^{-1}),

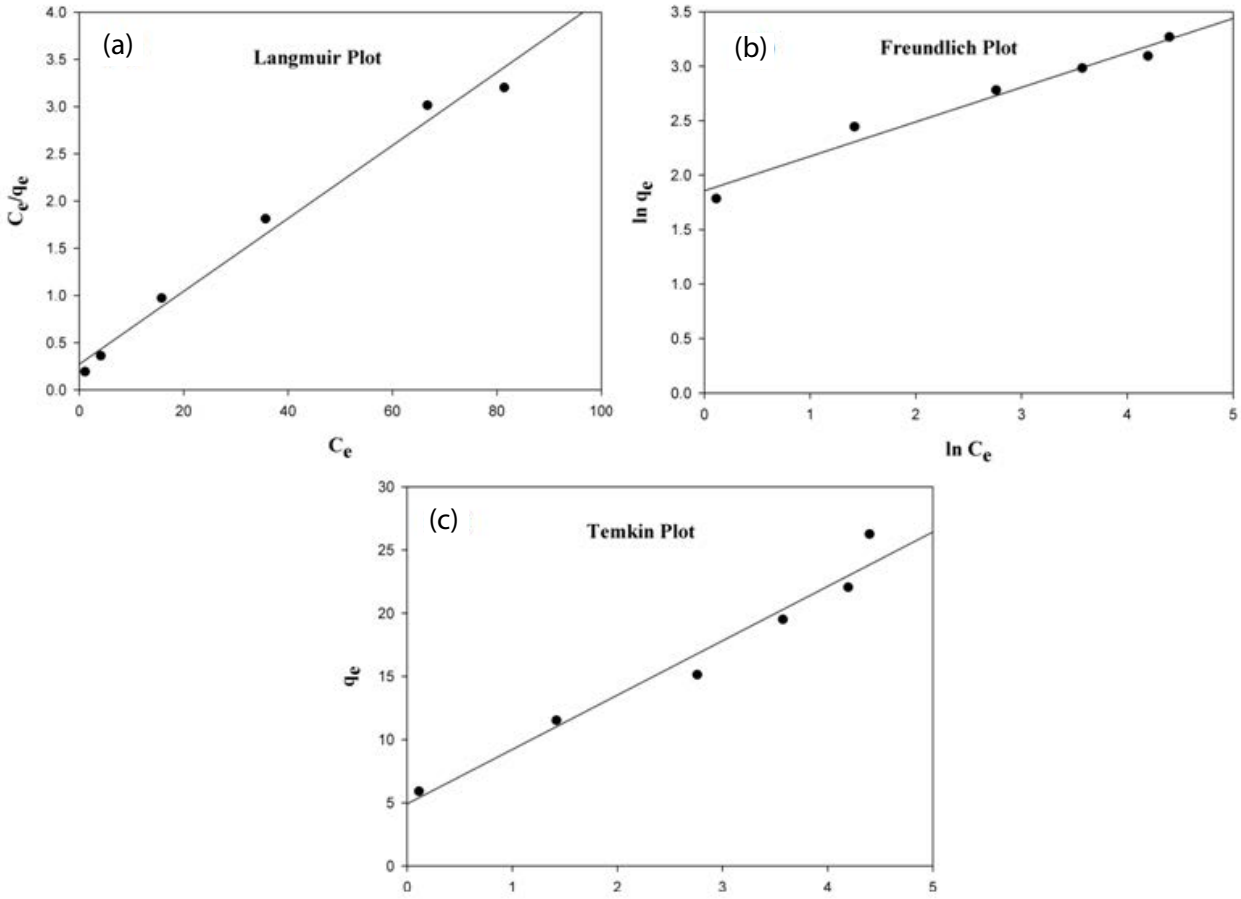

Fig. 8. Isotherm plots for RG 19 adsorption on AMTL at 30°C: (a) Langmuir model, (b) Freundlich model and (c) Temkin model.

Table 3
Isotherm constant values for RG 19 adsorption on AMTL at room temperature

Isotherm	Parameters	Parameters values	R^2
Langmuir	q_m (mg g^{-1})	26.316	0.988
	K_L (L mg^{-1})	7.132	
Freundlich	K_F (mg g^{-1})(L g^{-1})$^{1/n}$	6.398	0.971
	n	3.165	
Temkin	A (L g^{-1})	3.132	0.961
	B	4.302	

T (K) represents absolute temperature, b (J mol^{-1}) is the Temkin isotherm constant, A (L mg^{-1}) is the equilibrium binding constant. The values of A, B and linear regression correlation (R^2) for Temkin isotherm model are given in Table 3.

It can be easily seen from Fig. 8a that the Langmuir isotherm fits the equilibrium data better than Freundlich and Temkin isotherms. The higher R^2 value also confirms that the Langmuir isotherm is fitted better with equilibrium data than Freundlich and Temkin isotherms. Moreover from Table 3, it is manifested that the predicted q_m value from the Langmuir model at initial dye concentration of 100 ppm is almost equivalent to our experimental q_m value showing mere 0.3% deviation among them. For the adsorption of RG 19 by AMTL with initial dye concentration of 100 ppm, R_L value was calculated as 1.4×10^{-3} (in the range of $0 < R_L < 1$) revealing the favourability of the adsorption phenomenon. Furthermore the value of 'n' from Freundlich isotherm was determined as 3.165 (>1), which also indicated the appropriateness of RG 19 adsorption by AMTL. Therefore the adsorption of RG 19 on AMTL was contemplated to be as monolayer adsorption with homogenous surface affinity.

3.8. Dye biosorption kinetics

In order to determine the biosorption kinetics of RG 19 on AMTL for the simulated solution, Lagergren pseudo-first-order model and pseudo-second-order kinetic model were applied to the experimental data. These two models are the most common models for the determination of adsorption kinetics. Linear regression correlation coefficient (R^2) values were utilized for the selection of the best fitted model.

3.8.1. Pseudo-first-order

The Lagergren pseudo-first-order model suggests a proportional adsorption rate and widely applied for the

adsorption of solute from its liquid solution. The pseudo-first-order model was suggested by Lagergren [56] as follows:

$$\log(q_e - q_t) = \log(q_e) - \left(\frac{k_1}{2.303}\right)t \quad (11)$$

where k_1 (1 min^{-1}) is the pseudo-first-order adsorption rate constant. The pseudo-first-order adsorption rate constant (k_1) and q_e values can be calculated by plotting log ($q_e - q_t$) vs. time (figure not shown) at different dye concentrations [57]. The values of k_1, q_e and corresponding linear regression correlations (R^2) values are shown in Table 4.

3.8.2. Pseudo-second-order

The pseudo-second-order rate expression can be expressed in the form of Eq. (12) [58].

$$\frac{t}{q_t} = \frac{1}{k_2 q_e^2} + \frac{t}{q_e} \quad (12)$$

where k_2 (g mg^{-1} min^{-1}) is the constant for pseudo-second-order adsorption. The values of k_2 and equilibrium adsorption capacity (q_e) can be calculated from the slope and intercept of t/q_t vs. t plot (Fig. 9). The values of determined k_2, q_e and R^2 values are shown in Table 4.

The linear regression correlation (R^2) values for pseudo-second-order kinetic model were found to be higher than the R^2 values for pseudo-first-order kinetic model. It is also easily found from Table 4 that the calculated values ($q_{e,\text{cal}}$) are close to experimental values ($q_{e,\text{exp}}$) for pseudo-second-order kinetic model. Therefore adsorption kinetics of RG 19 on AMTL can be convincingly described by pseudo-second-order kinetic model in comparison with the pseudo-first-order model.

3.9. Intraparticle diffusion

The previously described kinetic models could not define the dye diffusion mechanism; hence intraparticle diffusion model proposed by Weber and Morris [59] was considered in the present study to describe dye adsorption mechanism using AMTL. The empirical equation for intraparticle mechanism proposed by Weber and Morris is expressed as follows.

$$q_t = k_{\text{pi}} t^{1/2} + C_i \quad (13)$$

where k_{pi} (mg g^{-1} min$^{-1/2}$) is the intraparticle diffusion rate constant for the i th stage and C_i is the intercept related to the boundary layer thickness. The boundary layer effect increases with larger intercept. The values of k_{pi} and C_i can be obtained from the slope and the intercept of q_t vs. $t^{1/2}$ straight line (Fig. 10). If q_t vs. $t^{1/2}$ gives linear plot then the intraparticle diffusion is involved in the adsorption process and also if the straight line passes through the origin then the rate-limiting step in the adsorption process is solely governed by intraparticle diffusion [60]. Fig. 10 shows that none of the plot passed through the origin and all plots were multilinear curves with respect to the initial dye concentration, which implies that two or more steps control the adsorption process such as film diffusion followed by intraparticle diffusion in macro-, meso-, and micropores [61]. The values of intraparticle diffusion parameters and linear regression correlations (R^2) for all the linear stages are presented in Table 5. The initial sharper region of the plots is mostly due to the diffusion of dye molecules through the film to the external surface of the biosorbent (film diffusion) and the second portion exhibits the diffusion of the dye molecules within the pores of the biosorbent (intraparticle diffusion). The two phases in Fig. 10 imply that the biosorption of RG 19 involved surface biosorption and intraparticle diffusion. The first phase of adsorption was completed within 16 min, for all dye concentrations, and

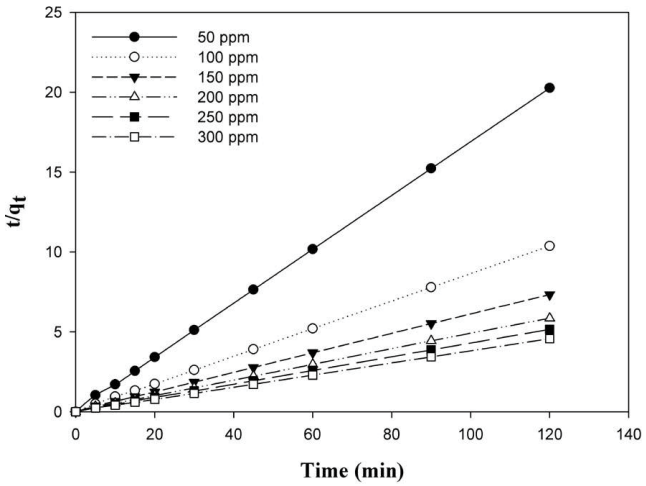

Fig. 9. Pseudo-second-order model for RG 19 on AMTL for different initial concentrations at 30°C.

Table 4
Kinetic parameters values for the removal of RG 19 at room temperature

Initial concentration (mg L^{-1})	$q_{e,\text{exp}}$ (mg g^{-1})	Pseudo-first-order kinetic model			Pseudo-second-order kinetic model		
		k_1 (1 min^{-1})	$q_{e,\text{cal}}$ (mg g^{-1})	R^2	k_2 (g mg^{-1} min^{-1})	$q_{e,\text{cal}}$ (mg g^{-1})	R^2
50	5.923	0.049	0.419	0.540	0.487	5.93	0.999
100	11.57	0.064	1.267	0.712	0.207	11.61	0.999
150	16.357	0.052	2.262	0.707	0.108	16.42	0.999
200	20.5	0.041	3.670	0.645	0.052	20.57	0.998
250	23.26	0.078	5.642	0.904	0.055	23.41	0.999
300	26.24	0.064	3.805	0.744	0.065	26.38	0.999

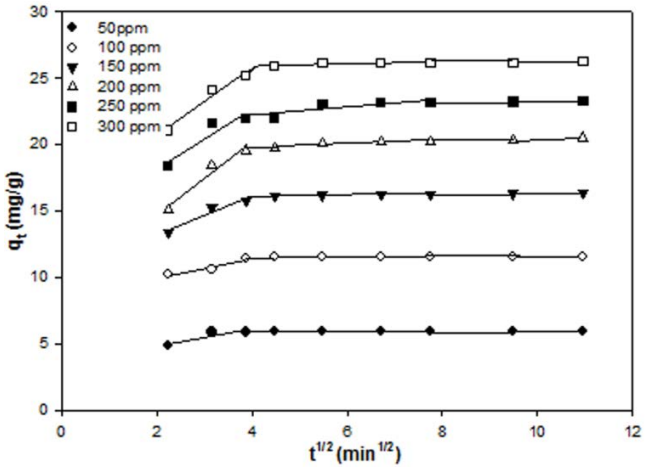

Fig. 10. Intraparticle diffusion plot for RG 19 adsorption on AMTL for different initial concentrations at 30°C.

then intraparticle diffusion observed in the second phase. The nonlinearity of the plots (Fig. 10) over the complete time scale implies that more than one process involved for RG 19 dye biosorption.

3.10. Characterisation of raw, modified and dye-loaded used tea leaves

3.10.1. Thermogravimetric and X-ray analysis

Thermogravimetric analysis (TGA) was performed using PerkinElmer, Singapore, analyser under nitrogen atmosphere with 150 mL min^{-1} flow rate, 15°C min^{-1} temperature increasing rate and platinum crucible with alpha alumina powder as reference. The analysis was performed in the temperature range of 34°C–800°C. Fig. 11a shows the thermal stability of both raw used tea leaves and AMTL under the above-mentioned conditions. Comparative study of TGA between raw and modified tea leaves does not indicate any significant deviation in thermal stability before and after acid treatment of the biosorbent, only manifesting slight improvement in terms of reduced weight loss after biosorbent modification. Tea leaves is a lignocellulosic compound consisting mainly cellulose, hemicellulose and lignin components. The TGA for AMTL initially shows only 8% weight loss with the gradual increase in temperature up to 100°C due to the loss of hygroscopic water content from the sample. The onset of biosorbent decomposition is clearly marked by the weight loss starting from 240°C because of the breakdown of hemicellulose content of

Table 5
Intraparticle diffusion model constants and correlation coefficients for the adsorption of RG 19 on AMTL for different initial concentrations at 30°C

Initial concentration (mg L^{-1})	First stage adsorption			Second stage adsorption		
	k_{p1} (mg g^{-1} $min^{-1/2}$)	C_1	R_1^2	k_{p2} (mg g^{-1} $min^{-1/2}$)	C_2	R_2^2
50	0.644	3.5298	0.8152	0.009	5.827	0.9714
100	0.6933	8.5535	0.8972	0.0099	11.461	0.9647
150	1.4714	10.261	0.9441	0.0339	15.992	0.9592
200	2.7796	9.0805	0.9563	0.1474	19.169	0.7911
250	2.238	13.737	0.8737	0.3218	20.918	0.6707
300	2.5568	15.578	0.9595	0.0794	25.598	0.7514

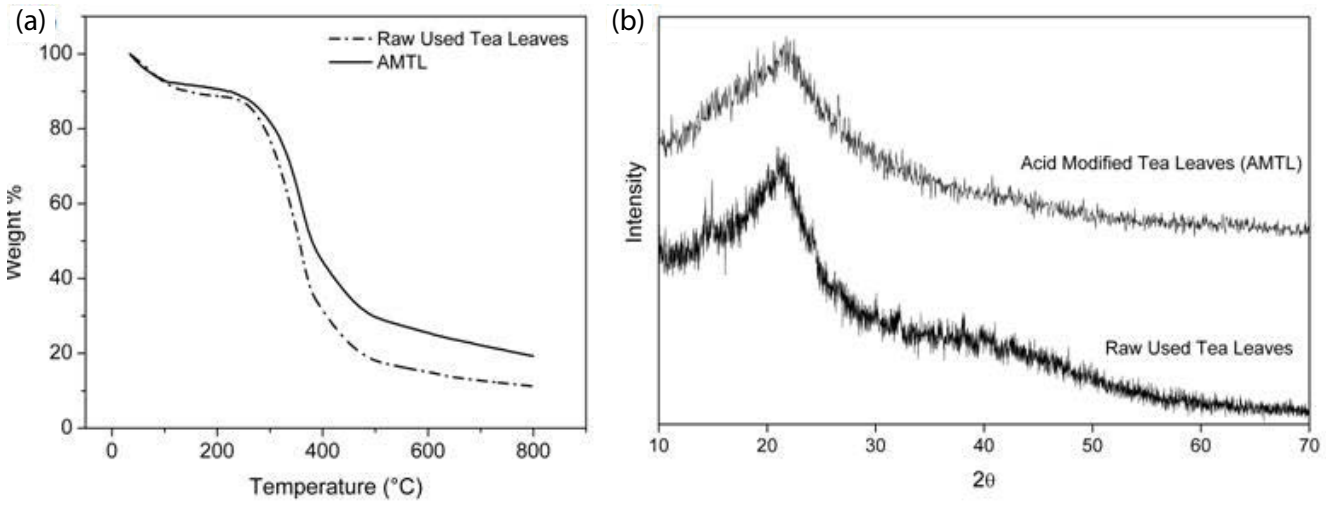

Fig. 11. (a) TGA plot for both raw used tea leaves and AMTL as biosorbent and (b) XRD plot for both raw used tea leaves and AMTL as biosorbent.

the used tea leaves. Beyond 240°C, the rate of weight loss increases rapidly and continues up to 300°C because of the decomposition of hemicelluloses. Again the rate of change in weight loss gets elevated because of the cellulose decomposition and reaches the maximum value at 445°C when the major fraction of cellulose content decomposes and lignin part starts to decay. After 445°C, the biosorbent loss becomes continuous due to conversion of the biosorbent into oxides with any further increase in temperature. This thermal stability analysis of AMTL suggests that AMTL can be successfully used as a biosorbent in various industries at an elevated temperature.

X-ray analysis of both raw used tea leaves and AMTL was performed to determine whether the biosorbent is amorphous or crystalline in nature. In Fig. 11b, a diffraction peak is observed at around 2θ = 22.5° which helps to portray the characteristic of raw used tea leaves and AMTL. For raw used tea leaves, the XRD pattern shows peaks at around 2θ = 17° revealing the amorphous portion (such as cellulose, hemicellulose and lignin) and at 2θ = 22.5° indicating the presence of partially crystallized fraction of cellulose. However, XRD analysis of AMTL shows no significant high or middle intensity peaks, denoting the predominant amorphous nature of AMTL. At 2θ = 22.5°, the diffraction peak was observed quite sharp for raw tea leaves but disappeared in acid-modified samples. Therefore the absence of any characteristic peaks on XRD pattern after acid treatment manifests the turbostratic structure of disordered carbonaceous materials in the sample, compared with raw tea leaves.

3.10.2. FT-IR analysis of raw, modified and dye-loaded used tea leaves

The FT-IR spectral analysis has been evaluated in details under the light of previous literatures and is shown in Fig. 12. The FT-IR analysis was carried out in the range of 400–4,000 cm^{-1} to determine the presence of different functional groups on the raw tea leaves, modified tea leaves surface before and after dye adsorption. The spectra portray several absorption peaks, inferring the complex nature of used tea leaves. The first observed peak at 3,414 cm^{-1} is referring to vibration of OH stretching which is quite stronger for the raw tea leaves. However this peak has been weakened for the modified tea leaves after the acid treatment. The bands showed at both 2,918 and 2,843 cm^{-1} in case of modified tea leaves before and after adsorption are ascribing to aliphatic C–H bands (asymmetric and symmetric, respectively), which are completely missing for the raw tea samples. Therefore it was concluded that with the aid of acid activation, phosphoric acid brings significant changes in the chemical structure of the raw tea leaves. At wave number range of 1,740–1,750 cm^{-1}, a shoulder can be observed which is assigned to the carbonyl stretch of carboxyl. Stretching absorption band at 1,740–1,750 cm^{-1} is assigned to carbonyl C=O which is observed for the raw material. During acid treatment, phosphoric acid participates to break some bonds in both aliphatic and aromatic compounds available in the raw tea leaves resulting in release and elimination of several volatile and light weight substrates and thereby inducing partial aromatisation. This described behaviour is confirmed with the almost complete desertion of C=O stretch at 1,738 cm^{-1} in the raw tea leaves [25]. The plateau observed at 1,630–1,650 cm^{-1} could be inferred as the C=O stretching when being conjugated with amine (NH_2 band). Moreover the bands highlighted in the range of 1,520–1,550 cm^{-1} indicate the presence of secondary amine group. The peaks noticed at 1,234 and 1,036 cm^{-1} are ascribed to $–SO_3$ stretching and C=O stretching of ether groups, respectively. Table 6 shows that some peaks are shifted after dye adsorption while some peaks retain the same position. Henceforth, the shift in functional groups of –OH, C=O, $–NH_2$, –CH in tea leaves before and after adsorption of dye suggests the probable interactions of these functional groups with RG 19, following the mechanism of hydrogen bonding, surface complex and electrostatic attraction.

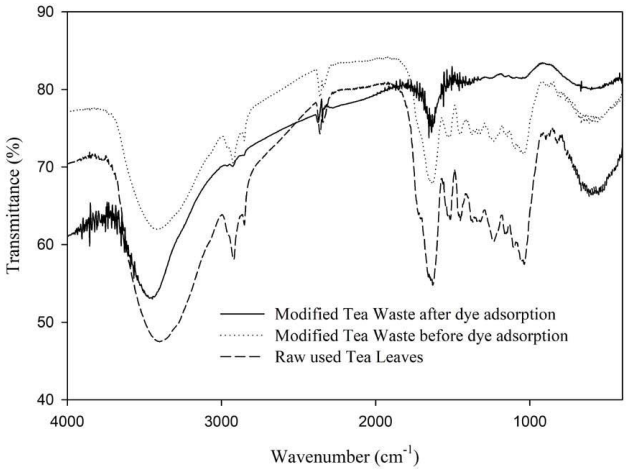

Fig. 12. Comparative FT-IR spectra analysis of raw used tea leaves, AMTL and dye-loaded AMTL biosorbent.

3.10.3. SEM micrographs of raw used tea leaves, AMTL and dye-loaded AMTL biosorbent

SEM images of the raw used tea leaves, modified tea leaves before and after dye biosorption are represented in Figs. 13a–c, respectively. It clearly indicates that the surface morphology of the raw used tea leaves (Fig. 13a) is comparatively smoother, posses reduced voids and cracks, whereas modified tea leaves after acid treatment (Fig. 13b) shows the presence of numerous cracks with high voids and a few grains of varied size distribution in large holes. Moreover the surface morphology of modified tea leaves is rather irregular, rough and heterogeneous in nature. However, after dye adsorption (Fig. 13c) the surface of AMTL is almost completely blanketed with dye molecules, affirming the occurrence of adsorption mechanism of dye molecules onto the pores of modified tea leaves.

The major constituents of the raw biosorbent, biosorbent before dye adsorption and after dye adsorption were analysed by EDX analysis. The major constituents of the raw used tea leaves were only C and O, without reflecting the presence of any inorganic metals (Fig. 13d). However after acid treatment, modified tea leaves before adsorption contain C (59.4%), O (38.65%) and P (1.95%) at very minor

Table 6
FT-IR spectral characteristics of AMTL before and after dye adsorption

IR peak	Frequency (cm^{-1})			Assignment
	Before adsorption	After adsorption	Differences	
1	3,414.02	3,422.07	+8.05	Bonded –OH group
2	2,918.76	2,926.8	+8.04	Aliphatic –C–H group
3	2,842.67	2,849.99	+7.73	Aliphatic –C–H group
4	2,362.77	2,354.72	–8.05	–C=N stretching
6	1,631.21	1,623.17	–8.04	–C=O stretching
7	1,517.09	1,524.41	+7.32	Secondary amine group
8	1,455.60	1,448.32	–7.28	Symmetric bending of CH_3
9	1,372.24	1,379.58	+7.34	Symmetric bending of CH_3
10	1,326.15	1,334.2	+8.05	Amine group
11	1,234.71	1,234.71	0	$–SO_3$ stretching
11	1,036.46	1,036.46	0	C=O stretching
12	891.607	899.655	8.048	–C–C– group
13	587.279	579.232	–8.047	–C–C– group

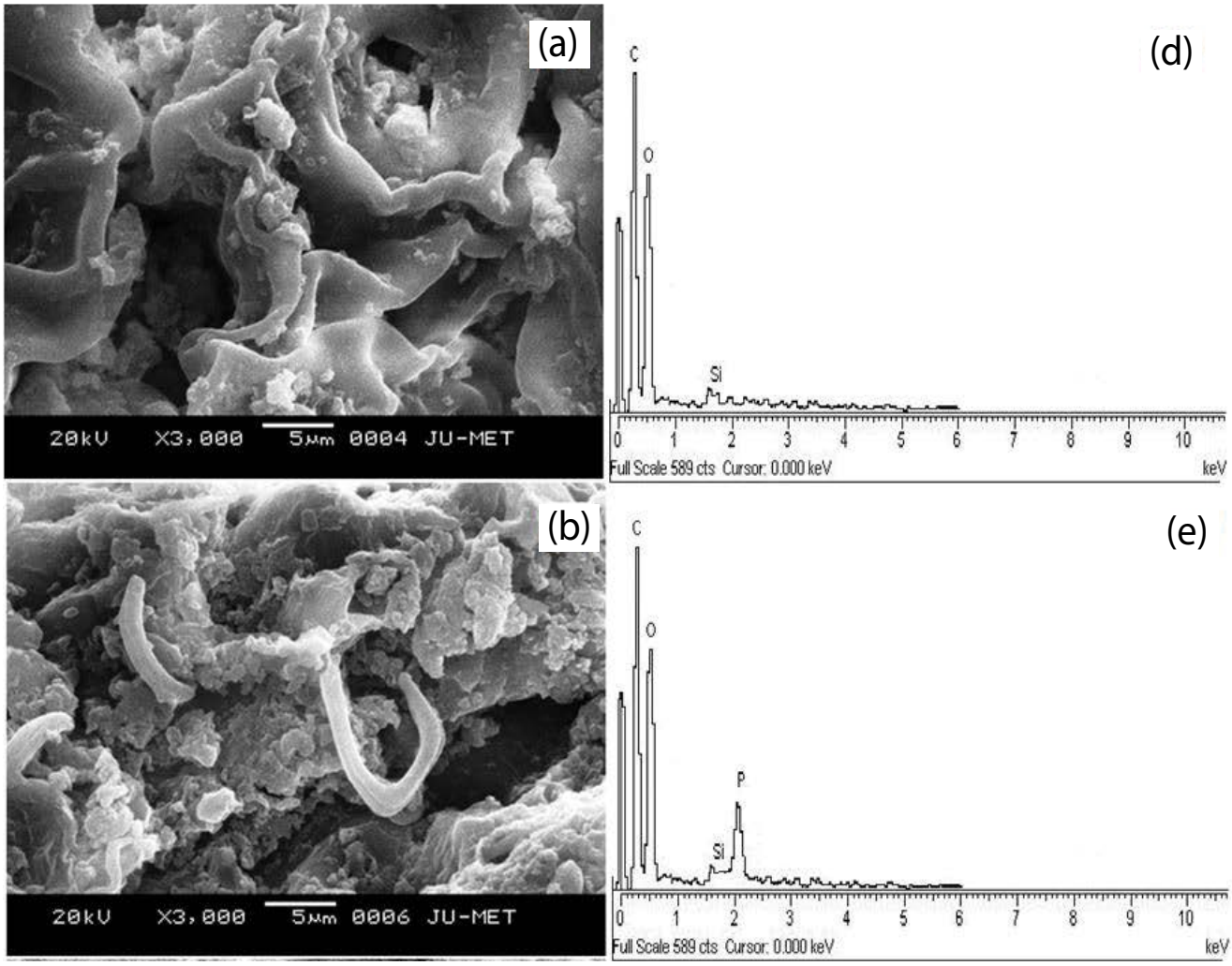

(*Fig. 13. Continued*)

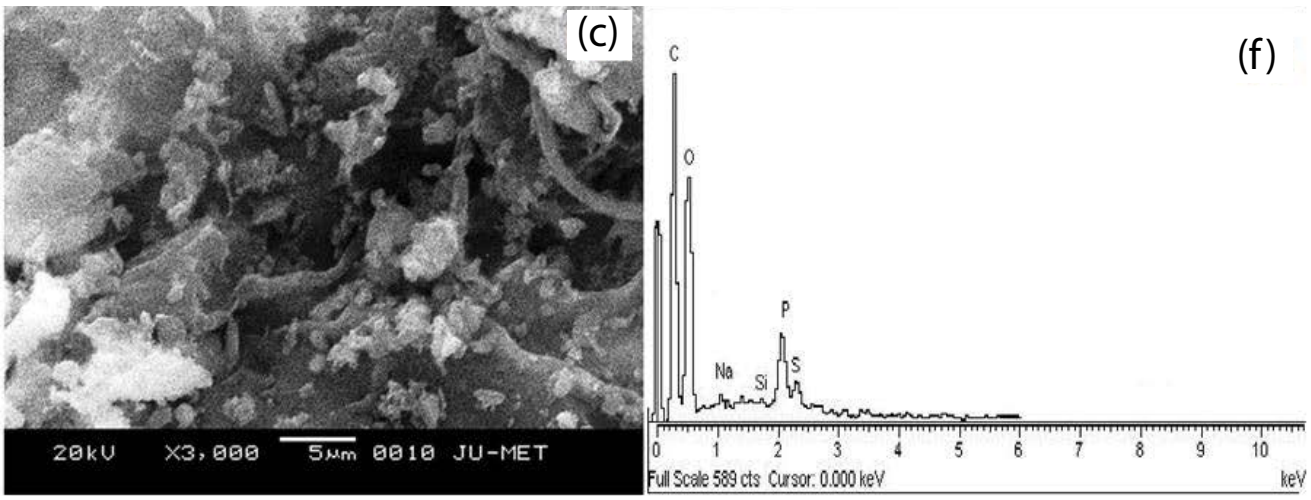

Fig. 13. SEM images for (a) raw used tea leaves, (b) AMTL before dye adsorption and (c) AMTL after dye adsorption. EDX spectra of (d) raw used tea leaves, (e) AMTL before dye adsorption and (f) AMTL after dye adsorption.

amount (Fig. 13e). The EDX analysis of modified tea leaves after dye adsorption (Fig. 13f) portrays the existence of Na (0.12%) and S (1.01%) peaks as sodium (Na) and sulphur (S) in the dye structure, confirming the attachment of the dye on the modified biosorbent. All the characterisation techniques support the modification of tea leaves during acid treatment and also confirmed the high adsorption capability of AMTL.

3.11. Regeneration and reusability of the biosorbent

One of the most important aspects of any adsorption process from economical and environmental perspective is the regeneration of the used biosorbent. The prime intricacy involved in adsorption processes is the disposal of used biosorbent. Therefore, regeneration of the used biosorbent can deflate the requirement of new biosorbent and even can diminish the difficulties related to disposal of used biosorbent. Henceforth in the present study, agricultural waste, that is, used tea leaves has been selected as the biosorbent considering the benefits of its usage such as less expensive, readily available, easy regeneration, high adsorption capacity, needs minor processing, etc. As used tea leaves are available worldwide at very low cost or no cost, the requirement of regeneration is not so demanding. Moreover considering the significant calorific value of used tea leaves of around 21.69 mJ kg^{-1}, these exhausted biosorbents can be easily disposed by incineration and utilizing the heat for steam generation [62,63].

However, desorption and reusability properties of the modified tea leaves were evaluated here to determine the stability of biosorbent. The reusability of AMTL towards adsorption of anionic dye RG 19 was experimented for three consecutive cycles. The biosorbent used in the biosorption of RG 19 solution (initial dye concentration of 100 mg L^{-1}) was separated from the solution via filtration process using Whatman filter paper. Then the dye-loaded AMTL were washed using distilled water to get rid of unadsorbed dye. Then the desorption was carried out by mixing this biosorbent into water and kept for shaking at stirring speed of 200 rpm for next 12 h at 30°C. After desorption, the biosorbent was again washed with distilled water for several times to remove any residual dye molecules followed by drying in hot air oven at 80°C. Reusability of AMTL was assessed by the change in removal percentage of RG 19 with the increase of reusage cycles as shown in Fig. 14. It has been observed that the removal rate has reduced from 95.9% to about 33% after three successive cycles. The gradual decrease in the removal capacity of desorbed AMTL is because of the alteration in superficial structure of modified tea leaves and blockage of the maximum binding sites in used tea leaves. Concurrently, it can be deduced from the experimental observations of desorption that AMTL has the potential to be considered as a promising biosorbent for RG 19 removal without causing any sort of secondary pollution.

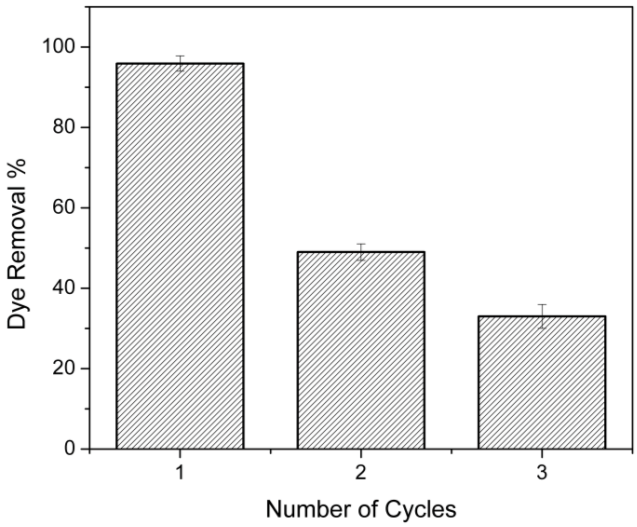

Fig. 14. Reusability of the biosorbent in terms of dye removal percentage with consecutive adsorption cycles.

4. Conclusions

In this present study, AMTL was used as an effective biosorbent for the removal of anionic dye RG 19 from aqueous solutions and AMTL can be used as inexpensive biosorbent for wastewater treatment. Langmuir, Freundlich and Temkin isotherm models were used for the analysis of the experimental data. It was observed that experimental data gave best fitting with the Langmuir isotherm with a monolayer adsorption capacity of 26.316 mg g^{-1}. The adsorption of RG 19 by AMTL followed pseudo-second-order kinetics with good correlation, R^2 = 0.999. The multilinear plots expressed that the dye adsorption process involved more than one adsorption mechanism. Hence AMTL can be utilised as an inexpensive biosorbent for removal of RG 19 from aqueous solution.

Acknowledgements

This research work was supported by University Grant Commission, India and Department of Science and Technology, India.

References

[1] Z. Hu, H. Chen, F. Ji, S. Yuan, Removal of Congo Red from aqueous solution by cattail root, J. Hazard. Mater., 173 (2010) 292–297.
[2] M.K. Purkait, A. Maiti, S. Dasgupta, S. De, Removal of congo red using activated carbon and its regeneration, J. Hazard. Mater., 145 (2007) 287–295.
[3] C.I. Pearce, J.R. Lloyd, J.T. Guthrie, The removal of colour from textile wastewater using whole bacterial cells: a review, Dyes Pigm., 58 (2003) 179–196.
[4] E. Forgacs, T. Cserhati, G. Oros, Removal of synthetic dyes from wastewaters: a review, Environ. Int., 30 (2004) 953–971.
[5] E. Bulut, M. Özacar, İ.A. Şengil, Equilibrium and kinetic data and process design for adsorption of Congo Red onto bentonite, J. Hazard. Mater., 154 (2008) 613–622.
[6] M.A.M. Salleh, D.K. Mahmoud, W.A.W.A. Karim, A. Idris, Cationic and anionic dye adsorption by agricultural solid wastes: a comprehensive review, Desalination, 280 (2011) 1–13.
[7] P. Nigam, G. Armour, I.M. Banat, D. Singh, R. Marchant, Physical removal of textile dyes from effluents and solid-state fermentation of dye-adsorbed agricultural residues, Bioresour. Technol., 72 (2000) 219–226.
[8] T. Robinson, B. Chandran, P. Nigam, Removal of dyes from a synthetic textile dye effluent by biosorption on apple pomace and wheat straw, Water Res., 36 (2002) 2824–2830.
[9] W. Azmi, R.K. Sani, U.C. Banerjee, Biodegradation of triphenylmethane dyes, Enzyme Microb. Technol., 22 (1998) 185–191.
[10] J. Sun, L. Qiao, S. Sun, G. Wang, Photocatalytic degradation of Orange G on nitrogen-doped TiO_2 catalysts under visible light and sunlight irradiation, J. Hazard. Mater., 155 (2008) 312–319.
[11] A. Durán, J.M. Monteagudo, E. Amores, Solar photo-Fenton degradation of Reactive Blue 4 in a CPC reactor, Appl. Catal., B, 80 (2008) 42–50.
[12] J. Garcia-Montano, N. Ruiz, I. Munoz, X. Domenech, J.A. Garcia-Hortal, F. Torrades, J. Peral, Environmental assessment of different photo-Fenton approaches for commercial reactive dye removal, J. Hazard. Mater., 138 (2006) 218–225.
[13] L. Fan, Y. Zhou, W. Yang, G. Chen, F. Yang, Electrochemical degradation of aqueous solution of Amaranth azo dye on ACF under potentiostatic model, Dyes Pigm., 76 (2008) 440–446.
[14] G. Sudarjanto, B. Keller-Lehmann, J. Keller, Optimization of integrated chemical-biological degradation of a reactive azo dye using response surface methodology, J. Hazard. Mater., 138 (2006) 160–168.
[15] A. Das, S. Mishra, Removal of textile dye reactive green-19 using bacterial consortium: process optimization using response surface methodology and kinetics study, J. Environ. Chem. Eng., 5 (2017) 612–627.
[16] B.H. Hameed, A.T.M. Din, A.L. Ahmad, Adsorption of methylene blue onto bamboo-based activated carbon: kinetics and equilibrium studies, J. Hazard. Mater., 141 (2007) 819–825.
[17] J. Tie, D. Chen, M. Zhao, X. Wang, S. Zhou, L. Peng, Adsorption of reactive green 19 from water using polyaniline/bentonite, J. Water Reuse Desalin., 6 (2016) 515–523.
[18] S. Mondal, Methods of dye removal from dye house effluent—an overview, Environ. Eng. Sci., 25 (2008) 383–396.
[19] A. Nath, S. Chakraborty, C. Bhattacharjee, Bioadsorbtion of industrial dyes from aqueous solution onto water hyacinth (*Eichornia crassipes*): equilibrium, kinetic, and sorption mechanism study, Desal. Water Treat., 52 (2014) 1484–1494.
[20] Y.-S. Ho, T.-H. Chiang, Y.-M. Hsueh, Removal of basic dye from aqueous solution using tree fern as a biosorbent, Process Biochem., 40 (2005) 119–124.
[21] L. Wang, A. Wang, Adsorption characteristics of Congo Red onto the chitosan/montmorillonite nanocomposite, J. Hazard. Mater., 147 (2007) 979–985.
[22] K.V. Kumar, A. Kumaran, Removal of methylene blue by mango seed kernel powder, Biochem. Eng. J., 27 (2005) 83–93.
[23] S.D. Khattri, M.K. Singh, Removal of malachite green from dye wastewater using neem sawdust by adsorption, J. Hazard. Mater., 167 (2009) 1089–1094.
[24] R. Gong, Y. Jin, F. Chen, J. Chen, Z. Liu, Enhanced malachite green removal from aqueous solution by citric acid modified rice straw, J. Hazard. Mater., 137 (2006) 865–870.
[25] R. Malik, D.S. Ramteke, S.R. Wate, Adsorption of malachite green on groundnut shell waste based powdered activated carbon, Waste Manage., 27 (2007) 1129–1138.
[26] A. Gürses, S. Karaca, Ç. Doğar, R. Bayrak, M. Açıkyıldız, M. Yalçın, Determination of adsorptive properties of clay/water system: methylene blue sorption, J. Colloid. Interface Sci., 269 (2004) 310–314.
[27] B. Acemioğlu, Adsorption of Congo red from aqueous solution onto calcium-rich fly ash, J. Colloid. Interface Sci., 274 (2004) 371–379.
[28] J.H. Tay, X.G. Chen, S. Jeyaseelan, N. Graham, Optimising the preparation of activated carbon from digested sewage sludge and coconut husk, Chemosphere, 44 (2001) 45–51.
[29] A.T.M. Din, B.H. Hameed, A.L. Ahmad, Batch adsorption of phenol onto physiochemical-activated coconut shell, J. Hazard. Mater., 161 (2009) 1522–1529.
[30] K. Ekta, K. Satindar, P.N. Dave, Surfactant modified tea waste as a novel adsorbent for the removal of basic dye, Der Chemica Sinica, 2 (2011) 87–102.
[31] O.S. Amuda, A.A. Giwa, I.A. Bello, Removal of heavy metal from industrial wastewater using modified activated coconut shell carbon, Biochem. Eng. J., 36 (2007) 174–181.
[32] A.M. Puziy, O.I. Poddubnaya, A. Martínez-Alonso, F. Suárez-García, J.M.D. Tascón, Surface chemistry of phosphorus-containing carbons of lignocellulosic origin, Carbon, 43 (2005) 2857–2868.
[33] F. Suárez-Garcıa, A. Martınez-Alonso, J.M.D. Tascón, Pyrolysis of apple pulp: chemical activation with phosphoric acid, J. Anal. Appl. Pyrolysis, 63 (2002) 283–301.
[34] V. Nathan, S. Sreenivas, Dynamics of India's tea production: an econometric analysis, Int. J. Sci. Res., 4 (2014).
[35] B.M.W.P.K. Amarasinghe, R.A. Williams, Tea waste as a low cost adsorbent for the removal of Cu and Pb from wastewater, Chem. Eng. J., 132 (2007) 299–309.
[36] Md.T. Uddin, M.A. Islam, S. Mahmud, Md. Rukanuzzaman, Adsorptive removal of methylene blue by tea waste, J. Hazard. Mater., 164 (2009) 53–60.
[37] V.K. Garg, M. Amita, R. Kumar, R. Gupta, Basic dye (methylene blue) removal from simulated wastewater by adsorption using Indian Rosewood sawdust: a timber industry waste, Dyes Pigm., 63 (2004) 243–250.

[38] A. Zuorro, R. Lavecchia, F. Medici, L. Piga, Spent tea leaves as a potential low-cost adsorbent for the removal of azo dyes from wastewater, Chem. Eng., 32 (2013) 19–24.
[39] A. Xavier, P. Muthuraman, Adsorption of Reactive Green and Reactive Red Dyes from the Aqueous Solution using Activated Carbons, Int. J. Sci. Res., 4 (2015) 454–459.
[40] H. Nadi, M. Alizadeh, M. Ahmadabadi, A.R. Yari, S. Hashemi, Removal of reactive dyes (green, orange, and yellow) from aqueous solutions by peanut shell powder as a natural adsorbent, Arch. Hyg. Sci., 1 (2012) 41–47.
[41] M. Ghaedi, H. Tavallali, M. Sharifi, S.N. Kokhdan, A. Asghari, Preparation of low cost activated carbon from Myrtus communis and pomegranate and their efficient application for removal of Congo red from aqueous solution, Spectrochim. Acta A Mol. Biomol. Spectrosc., 86 (2012) 107–114.
[42] D.N. Jadhav, A.K. Vanjara, Adsorption equilibrium study: removal of dyestuff effluent using sawdust, polymerized sawdust and sawdust carbon-I, Indian J. Chem. Technol., 11 (2004) 194–200.
[43] G. McKay, V.J.P. Poots, Kinetics and diffusion processes in colour removal from effluent using wood as an adsorbent, J. Chem. Technol. Biotechnol., 30 (1980) 279–292.
[44] Y. Guo, J. Zhao, H. Zhang, S. Yang, J. Qi, Z. Wang, H. Xu, Use of rice husk-based porous carbon for adsorption of Rhodamine B from aqueous solutions, Dyes Pigm., 66 (2005) 123–128.
[45] C. Namasivayam, D. Kavitha, Removal of Congo Red from water by adsorption onto activated carbon prepared from coir pith, an agricultural solid waste, Dyes Pigm., 54 (2002) 47–58.
[46] R. Gong, Y. Ding, M. Li, C. Yang, H. Liu, Y. Sun, Utilization of powdered peanut hull as biosorbent for removal of anionic dyes from aqueous solution, Dyes Pigm, 64 (2005) 187–192.
[47] C. C. Liu, M. Kuang-Wang, Y. S. Li, Removal of nickel from aqueous solution using wine processing waste sludge, Ind. Eng. Chem. Res., 44 (2005) 1438–1445.
[48] G. Alberghina, R. Bianchini, M. Fichera, S. Fisichella, Dimerization of Cibacron Blue F3GA and other dyes: influence of salts and temperature, Dyes Pigm., 46 (2000) 129–137.
[49] J. Germán-Heins, M. Flury, Sorption of Brilliant Blue FCF in soils as affected by pH and ionic strength, Geoderma, 97 (2000) 87–101.
[50] Y.S. Al-Degs, M.I. El-Barghouthi, A.H. El-Sheikh, G.M. Walker, Effect of solution pH, ionic strength, and temperature on adsorption behavior of reactive dyes on activated carbon, Dyes Pigm., 77 (2008) 16–23.
[51] B.K. Dutta, Principles of mass transfer and separation processes, Can. Soc. J. Chem. Eng., 87 (2009) 818–819.
[52] I. Langmuir, The adsorption of gases on plane surfaces of glass, mica and platinum, J. Am. Chem. Soc., 40 (1918) 1361–1403.
[53] K.R. Hall, L.C. Eagleton, A. Acrivos, T. Vermeulen, Pore- and solid-diffusion kinetics in fixed-bed adsorption under constant-pattern conditions, Ind. Eng. Chem. Fundam., 5 (1966) 212–223.
[54] H. Freundlich, The Adsorption in Physical Chemistry, Leipzig, 1906.
[55] Y. S. Ho, G. McKay, Sorption of dye from aqueous solution by peat, Chem. Eng. J., 70 (1998) 115–124.
[56] S. Lagergren, About the theory of so-called adsorption of soluble substances, Kungliga Sven. Vetenskapsakad. Handingarl, 24 (1898) 1–39.
[57] H. Yuh-Shan, Citation review of Lagergren kinetic rate equation on adsorption reactions, Scientometrics, 59 (2004) 171–177.
[58] G. Blanchard, M. Maunaye, G. Martin, Removal of heavy metals from waters by means of natural zeolites, Water Res., 18 (1984) 1501–1507.
[59] W.J. Weber, J.C. Morris, Kinetics of adsorption on carbon from solution, J. Sanit. Eng. Div., 89 (1963) 31–60.
[60] Y. Ho, G. McKay, The kinetics of sorption of basic dyes from aqueous solution by sphagnum moss peat, Can. Soc. J. Chem. Eng., 76 (1998) 822–827.
[61] A.E. Ofomaja, Intraparticle diffusion process for lead (II) biosorption onto mansonia wood sawdust, Bioresour. Technol., 101 (2010) 5868–5876.
[62] I. Gaballah, D. Goy, E. Allain, G. Kilbertus, J. Thauront, Recovery of copper through decontamination of synthetic solutions using modified barks, Metall. Mater. Trans. B, 28 (1997) 13–23.
[63] K.L. Wasewar, M. Atif, B. Prasad, I.M. Mishra, Adsorption of zinc using tea factory waste: kinetics, equilibrium and thermodynamics, CLEAN–Soil, Air, Water, 36 (2008) 320–329.